

Five-Coordinate Platinum(II) Hydrides Containing 1,1,4,7,10,10-Hexaphenyl-1,4,7,10-tetraphosphadecane as a Tetradentate Monometallic Ligand

Peter Brüggeller

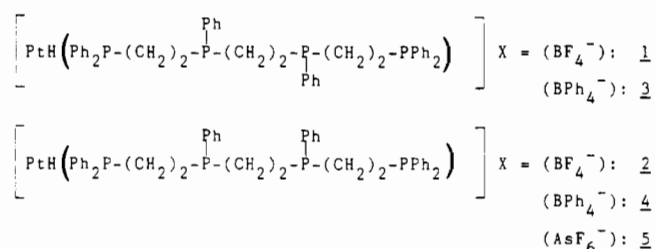
Received March 15, 1989

Five-coordinate platinum(II) hydrides have been prepared by NaBH_4 reduction of corresponding platinum(II) chlorides and tetracoordinate platinum(II) complexes, all coordination types containing 1,1,4,7,10,10-hexaphenyl-1,4,7,10-tetraphosphadecane (P_4) as a tetradentate monometallic ligand. Chiral $[\text{PtH}(\text{P}_4)](\text{BF}_4)$ (**1**), *meso*- $[\text{PtH}(\text{P}_4)](\text{BF}_4)$ (**2**), chiral $[\text{PtH}(\text{P}_4)](\text{BPh}_4)$ (**3**), and *meso*- $[\text{PtH}(\text{P}_4)](\text{BPh}_4)$ (**4**) have been characterized by elemental analyses, IR and NMR (^{195}Pt , ^{31}P , ^1H) spectroscopy, and an X-ray structure analysis. In **1** and **2** P_4 has a tetrahedral arrangement. The $^{31}\text{P}\{^1\text{H}\}$ NMR spectra of **1** and **2** indicate nearly identical magnetic environments for all four ^{31}P nuclei of P_4 , which are only partially resolved at 121.5 MHz. The 300-MHz ^1H NMR spectra show broad signals in the hydride region at 303 K and quintets at about 250 K. In **3** and **4** P_4 is coordinated in an intermediate geometry along the reaction coordinate between tetrahedral and square-planar structures. The proton-coupled ^{195}Pt NMR spectrum of **3** consists of 18 lines, produced by coupling of the ^{195}Pt nucleus with two equivalent PPh_2 groups, two equivalent PPh groups, and the hydride ligand. The $^{31}\text{P}\{^1\text{H}\}$ NMR spectra of **3** and **4** are consistent with A_2M_2 spin systems, both signals being split into triplets. In the hydride region the 300-MHz ^1H NMR spectra of **3** and **4** show triplets of triplets at 303 K, also indicating the presence of two equivalent PPh_2 and PPh groups, respectively. The solid-state structure of **3** deviates from its solution structure. An X-ray structure analysis has revealed a distorted trigonal-bipyramidal coordination of **3**: $\text{C}_{66}\text{H}_{63}\text{BP}_4\text{Pt}$, (hydrido)(1,1,4,7,10,10-hexaphenyl-1,4,7,10-tetraphosphadecane-*P,P',P'',P'''*)platinum(II) tetraphenylborate, $a = 12.126$ (3) Å, $b = 16.343$ (4) Å, $c = 16.390$ (6) Å, $\alpha = 74.31$ (3)°, $\beta = 76.02$ (2)°, $\gamma = 67.38$ (2)°, triclinic, $P\bar{1}$, $Z = 2$, $\text{Mo K}\alpha$, $\lambda = 0.71069$ Å, data collection in an $\omega/2\theta$ scan mode, structure solution by the heavy-atom method, refinement by least-squares procedures, and final $R = 0.066$. Solutions of *meso*- $[\text{PtH}(\text{P}_4)](\text{AsF}_6)$ (**5**) show an equilibrium between the two structural types **2** and **4** depending on the solvent. The ^{31}P and 300-MHz ^1H NMR spectra of acetone- d_6 solutions of **5** indicate the presence of an apical phosphorus atom trans to the hydride ligand, which is in agreement with the solid-state structure of **3**.

Introduction

Though several different types of five-coordinate Pt(II) centers in Pt(II) oligomers containing two or more hydride ligands are known,¹ stable five-coordinate monometallic platinum(II) hydrides are rare and have been found to be thermally unstable.² However, they can be stabilized by ligands that either electronically³ or sterically⁴ favor pentacoordinated Pt(II) and have been proposed to be key intermediates in catalytic olefin hydroformylation reactions.^{3a,5} Furthermore, platinum(II) coordination geometries other than square-planar that might react more rapidly or with different base pairs along a DNA chain are of interest for anti-tumor properties or metal labeling of DNAs.^{4c} In this paper several novel five-coordinate platinum(II) hydrides are reported that contain 1,1,4,7,10,10-hexaphenyl-1,4,7,10-tetraphosphadecane (P_4) as a tetradentate monometallic ligand. In this respect the ligand P_4 is of particular interest since it is flexible enough to allow different coordination types.⁶ Furthermore, four-coordinate

square-planar complexes of P_4 and platinum(II) appear to be destabilized,⁷ a condition that favors the formation of nonplanar structures releasing the strain in the equatorial plane.⁸ As a consequence, five-coordinate platinum(II) hydrides of the general formula $[\text{PtH}(\text{P}_4)]\text{X}$, where X^- is a noncoordinating anion, show different arrangements of P_4 depending on X. P_4 is tetrahedrally coordinated in $[\text{PtH}(\text{P}_4)](\text{BF}_4)$ (chiral, **1**; *meso*, **2**) as well as in an intermediate manner along the reaction coordinate between tetrahedral and square-planar structures in $[\text{PtH}(\text{P}_4)](\text{BPh}_4)$ (chiral, **3**; *meso*, **4**) and further leads to trigonal-bipyramidal coordinations in the solid-state structure of **3** and in *meso*- $[\text{PtH}(\text{P}_4)](\text{AsF}_6)$ (**5**).



Experimental Section

Reagents and Chemicals. Reagent grade chemicals were used as received unless stated otherwise. 1,1,4,7,10,10-Hexaphenyl-1,4,7,10-tet-

- (1) (a) Carmichael, D.; Hitchcock, P. B.; Nixon, J. F.; Mathey, F.; Pidcock, A. Presented at the Third International Conference on the Chemistry of the Platinum Group Metals, Sheffield, U.K., 1987; A-35. (b) Knobler, C. B.; Kaesz, H. D.; Minghetti, G.; Bandini, A. L.; Banditelli, G.; Bonati, F. *Inorg. Chem.* **1983**, *22*, 2324. (c) Bachechi, F.; Bracher, G.; Grove, D. M.; Kellenberger, B.; Pregosin, P. S.; Venanzi, L. M.; Zambonelli, L. *Inorg. Chem.* **1983**, *22*, 1031. (d) Paonessa, R. S.; Troglor, W. C. *Inorg. Chem.* **1983**, *22*, 1038. (e) Venanzi, L. M. *Coord. Chem. Rev.* **1982**, *43*, 251. (f) Brown, M. P.; Cooper, S. J.; Frew, A. A.; Manojlović-Muir, L.; Muir, K. W.; Puddephatt, R. J.; Thomson, M. A. *J. Organomet. Chem.* **1980**, *198*, C33.
- (2) Gerlach, D. H.; Kane, A. R.; Parshall, G. W.; Jesson, J. P.; Muetterties, E. L. *J. Am. Chem. Soc.* **1971**, *93*, 3543.
- (3) (a) Scriveranti, A.; Berton, A.; Toniolo, L.; Botteghi, C. *J. Organomet. Chem.* **1986**, *314*, 369. (b) Pregosin, P. S.; Rüegger, H. *Inorg. Chim. Acta* **1984**, *86*, 55. (c) Ammann, C.; Pregosin, P. S.; Scriveranti, A. *Inorg. Chim. Acta* **1989**, *155*, 217.
- (4) (a) Brüggeller, P. *Inorg. Chim. Acta* **1987**, *129*, L27. (b) Gieren, A.; Brüggeller, P.; Hofer, K.; Hübner, Th.; Ruiz-Pérez, C. *Acta Crystallogr., Sect. C* **1989**, *45*, 196. (c) Winter, J. A.; Lin, F. T.; Shepherd, R. E. *Inorg. Chim. Acta* **1989**, *155*, 155. (d) Dixon, K. R. *Inorg. Chem.* **1977**, *16*, 2618.
- (5) Petrosyan, V. S.; Permin, A. B.; Bogdashkina, V. I.; Krut'ko, D. P. *J. Organomet. Chem.* **1985**, *292*, 303.

- (6) (a) Brüggeller, P. *Inorg. Chim. Acta* **1989**, *155*, 45. (b) Stiegman, A. E.; Goldman, A. S.; Philbin, C. E.; Tyler, D. R. *Inorg. Chem.* **1986**, *25*, 2976. (c) Rivera, A. V.; De Gil, E. R.; Fontal, B. *Inorg. Chim. Acta* **1985**, *98*, 153. (d) Hale, A. L.; Jewiss, H. C.; Levason, W. *Inorg. Chim. Acta* **1985**, *97*, 85. (e) Brown, J. M.; Canning, L. R. *J. Organomet. Chem.* **1984**, *267*, 179. (f) Bacci, M.; Ghilardi, C. A.; Orlandini, A. *Inorg. Chim. Acta* **1984**, *23*, 2798. (g) Ghilardi, C. A.; Midollini, S.; Sacconi, L.; Stoppioni, P. *J. Organomet. Chem.* **1981**, *205*, 193. (h) Puttfarcken, U.; Rehder, D. *J. Organomet. Chem.* **1980**, *185*, 219. (i) Butler, I. S.; Coville, N. J. *J. Organomet. Chem.* **1974**, *66*, 111. (j) Bacci, M.; Ghilardi, C. A. *Inorg. Chim. Acta* **1974**, *13*, 2398.
- (7) Brüggeller, P.; Hübner, Th. Unpublished results.
- (8) (a) De Felice, V.; Ganis, P.; Vitagliano, A. *Inorg. Chim. Acta* **1988**, *144*, 57. (b) Atwood, J. D. *Inorganic and Organometallic Reaction Mechanisms*; Brooks/Cole: Monterey, CA, 1985; p 244.

Table I. ^{195}Pt (for **3**) and $^{31}\text{P}\{^1\text{H}\}$ NMR Data for Chiral and *meso*-[PtCl(P₄)](BF₄) and **1**–**5**^a

compd	$\delta(\text{P})$	$^1J(\text{Pt,P})$	compd	$\delta(\text{P})$	$^1J(\text{Pt,P})$		
chiral [PtCl(P ₄)](BF ₄)	46.5, 45.5, 43.9	2314, 2230, 2399	1	28.8, 24.7	1968, 2015		
<i>meso</i> -[PtCl(P ₄)](BF ₄)	43.1, 41.4, 38.0	2278, 2369, 2231	2	30.9, 24.7	2079, 2126		
compd	$\delta(\text{Pt})$	$^1J(\text{Pt,H})$	$\delta(\text{PPh})$	$\delta(\text{PPh}_2)$	$^1J(\text{Pt,PPh})$	$^1J(\text{Pt,PPh}_2)$	$^2J(\text{PPh,PPh}_2)$
3	(-5443 (tt) ^b)	701	64.6 (t)	23.0 (t)	2005	2676	80
4			62.1 (t)	21.1 (t)	1990	2699	82
5a ^c type 4			64.6 (t)	23.3 (t)	1992	2701	82
5b type 4			44.3 (t)	35.1 (t)	≈0	≈0	46
compd	$\delta(\text{P})$	$^1J(\text{Pt,P})$	compd	$\delta(\text{P})$	$^1J(\text{Pt,P})$		
5a type 2	30.9, 24.7	2080, 2125	5b type 2	28.6	2016		
compd	$\delta(\text{P}_{\text{ap}})$	$\delta(\text{P}_{\text{eq}})$	$^1J(\text{Pt,P}_{\text{ap}})$	$^1J(\text{Pt,P}_{\text{eq}})$	$^2J(\text{P}_{\text{eq}},\text{P}_{\text{ap}})$		
5a Berry process	91.9		2280 (283 K)				
5b Berry process	101.8 (d)	50.6 (d)	1859	2608	34		

^a J values in Hz. Spectra were run at 300 K; except for **3** and **4** (CH₂Cl₂, 32.4 MHz) and **5b** (acetone-*d*₆, 121.5 MHz) spectra were measured in CD₃NO₂ at 121.5 MHz. CD₃NO₂ solutions of chiral and *meso*-[PtCl(P₄)](BF₄), **1**, and **2** show solvolysis effects on standing, which are much slower if an excess of NaBF₄ is added to the solutions. ^btt = triplet of triplets, t = triplet, d = doublet; eq = equatorial, ap = apical. ^cThe signals corresponding to the intermediates between structural types **4** and **2** occur at $\delta(\text{PPh}) = 60.2$ ppm ($^1J(\text{Pt,PPh}) = 1695$ Hz) and $\delta(\text{PPh}_2) = 16.6$ ppm ($^1J(\text{Pt,PPh}_2) \approx 0$) and -5.5 ppm ($^1J(\text{Pt,PPh}_2) = 2693, 1214$ Hz) for **5a** and at $\delta(\text{PPh}_2) = 24.3$ ppm ($^1J(\text{Pt,PPh}_2) \approx 0$) and 11.3 ppm ($^1J(\text{Pt,PPh}_2) = 2892$ Hz) for **5b**. ³¹P 2D exchange experiments (which have not been conclusive with solutions of **5**, where the involved signals are too broad) with related [PtR(*meso*-P₄)]X (R = alkyl, X = noncoordinating anion) compounds showing a similar solution behavior have confirmed that **5** is an exchanging single species in solution.³⁰

raphosphadecane (P₄) was purchased from Strem Chemical Co. NaBH₄ (99.9%) was obtained from Fluka. LiAsF₆ was purchased from Ventron, and NaBF₄ from Fluka. Na(BPh₄) was of purissimum grade quality and was received from Merck-Schuchardt. Absolute ethanol and other organic solvents were obtained from Fluka. Solvents used for NMR measurements and for crystallization purposes were of purissimum grade quality. Na₂PtCl₄·4H₂O was prepared from platinum metal.

Instrumentation. Fourier-mode ^{195}Pt , ^{31}P , and ^1H NMR spectra were obtained by use of Bruker WP-80 (internal deuterium lock) and Bruker AM-300 (external deuterium lock) spectrometers and were recorded at 17.2, 32.4, and 121.5, and 300 MHz, respectively. Positive chemical shifts are downfield from 1.0 M Na₂PtCl₆ (external), 85% H₃PO₄ (external), and Me₄Si (internal) used as standards.

The X-ray data collection and analysis were performed on an Enraf-Nonius CAD4 diffractometer and a VAX computer.

Infrared spectra of solid complexes in KBr pellets were recorded with a Pye Unicam SP3-300 spectrometer from 4000 to 200 cm⁻¹. All hydride complexes showed strong absorptions in the typical Pt–H stretching region above 2000 cm⁻¹ and several strong absorptions below 1500 cm⁻¹.

Elemental analyses were obtained with a Heraeus EA 425 elemental analyzer.

Separation of the Stereoisomers of P₄. Commercial P₄ was separated by fractional crystallization to give the pure chiral and *meso* diastereomers, respectively, according to ref 6e.

Syntheses of Platinum(II) Complexes. A Schlenk apparatus and oxygen-free, dry Ar were used in the syntheses of all complexes. Solvents were degassed by several freeze–pump–thaw cycles prior to use.

Chiral and *meso*-[PtCl(P₄)](BF₄). The complexes were prepared according to ref 6a, where chiral and *meso*-P₄ were used, respectively, instead of commercial P₄. Chiral [PtCl(P₄)](BF₄): mp 195 °C. Anal. Calcd for C₄₂H₄₂BClF₄P₄Pt: C, 51.1; H, 4.3. Found: C, 50.9; H, 4.0. *meso*-[PtCl(P₄)](BF₄): mp 198 °C. Anal. Calcd for C₄₂H₄₂BClF₄P₄Pt: C, 51.1; H, 4.3. Found: C, 50.8; H, 4.1.

***meso*-[PtCl(P₄)](AsF₆).** The complex was also prepared according to ref 6a, where pure *meso*-P₄ and 0.6 mmol of LiAsF₆ instead of NaBF₄ were used. After recrystallization from CH₃NO₂: yield 0.196 g (60%); mp 190–193 °C dec. Anal. Calcd for C₄₂H₄₂AsClF₆P₄Pt: C, 46.3; H, 3.9. Found: C, 46.0; H, 3.7.

***meso*-[PtCl(P₄)](BPh₄), *meso*-[Pt(P₄)](BPh₄)₂, and chiral [Pt(P₄)](BPh₄)₂** were prepared according to ref 6a; it is also possible to get *meso*-[PtCl(P₄)](BPh₄) and chiral [Pt(P₄)](BPh₄)₂ by use of pure *meso*-P₄ and chiral P₄, respectively, according to ref 6a.

1 and 2. Chiral or *meso*-[PtCl(P₄)](BF₄) (0.198 g, 0.200 mmol), respectively, and NaBF₄ (0.044 g, 0.40 mmol) were suspended in 2.5 mL of absolute EtOH at 273 K. Under stirring, NaBH₄ (0.023 g, 0.60 mmol) was added in small portions. The slurry was stirred for 30 min, and its yellow color intensified. The suspension was allowed to warm to room temperature, and 5 mL of H₂O was added. The yellow precipitate was filtered off, washed several times with H₂O and 1:2 EtOH/H₂O, and dried in vacuo. **1**: yield 0.172 g (90%); mp 151 °C dec. Anal. Calcd for C₄₂H₄₃BF₄P₄Pt: C, 52.9; H, 4.5. Found: C, 52.6; H, 4.7. **2**: yield 0.165 g (86%); mp 132–135 °C dec. Anal. Calcd for C₄₂H₄₃BF₄P₄Pt: C, 52.9; H, 4.5. Found: C, 52.7; H, 4.6.

3 and 4. Chiral or *meso*-[Pt(P₄)](BPh₄)₂ (0.301 g, 0.200 mmol), respectively, was suspended in 5 mL of absolute EtOH at 293 K. Under stirring, NaBH₄ (0.023 g, 0.60 mmol) was added in small portions. The slurry was stirred for 3 h and turned slightly yellowish. After addition of 5 mL of H₂O the yellowish precipitate was filtered off, washed several times with H₂O and 1:2 EtOH/H₂O, and dried in vacuo. **3** was recrystallized from CH₂Cl₂: yellowish prisms yield 0.178 g (75%); mp 115–117 °C dec. Anal. Calcd for C₆₆H₆₃BP₄Pt: C, 66.8; H, 5.35. Found: C, 66.5; H, 5.5. **4**: yield 0.210 g (89%); mp 128–132 °C dec. Anal. Calcd for C₆₆H₆₃BP₄Pt: C, 66.8; H, 5.35. Found: C, 66.4; H, 5.6.

Analogous reduction of *meso*-[PtCl(P₄)](BPh₄) in 80% yield leads to no pure product (see results).

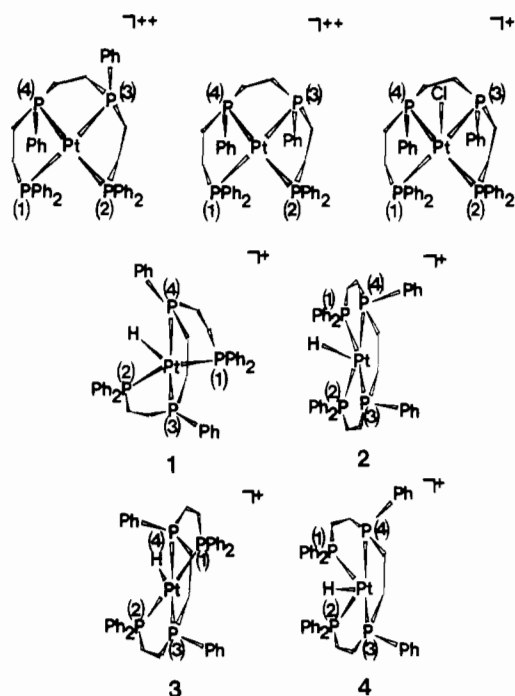
5. *meso*-[PtCl(P₄)](AsF₆) (0.218 g, 0.200 mmol) and LiAsF₆ (0.078 g, 0.40 mmol) were suspended in 2.5 mL of absolute EtOH at 293 K. Under stirring, NaBH₄ (0.023 g, 0.60 mmol) was added in small portions. The slurry was stirred for 30 min, and its yellow color intensified. After addition of 5 mL of H₂O the yellow precipitate was filtered off, washed several times with H₂O and 1:2 EtOH/H₂O, and dried in vacuo: yield 0.184 g (87%); mp 190–193 °C dec. Anal. Calcd for C₄₂H₄₃AsF₆P₄Pt: C, 47.8; H, 4.1. Found: C, 47.5; H, 4.1.

Results

Syntheses. The complexes **1**–**5** (Chart I) have been prepared by NaBH₄ reduction of five-coordinate platinum(II) chlorides and tetracoordinate platinum(II) complexes, all compounds containing P₄ as a tetradentate monometallic ligand. Though NaBH₄ reduction of neutral platinum(II) complexes usually leads to Pt(II) hydrides,^{9a} the reaction pathway may depend on the kind of counterion present, if cationic species are involved.^{1d,9b–d} In the above case reduction of [PtCl(P₄)]Cl and [Pt(P₄)]Cl₂ with NaBH₄ leads to the corresponding platinum(0) complex [Pt(P₄)].^{6a,10} Platinum(II) hydrides were formed only if noncoordinating anions instead of chloride are present. Furthermore, it depends on the coordination type of P₄ which platinum(II) hydride is produced. The two diastereomeric forms of [PtCl(P₄)](BF₄) both containing tetrahedrally coordinated P₄ (compare Table I) lead to **1** and **2**, where the coordination type of P₄ remains the same (see later). The two diastereomers of [Pt(P₄)](BPh₄)₂ show a square-planar arrangement of P₄.^{6a} However, their NaBH₄ reduction changes the coordination type of P₄ and **3** and **4** are formed containing nonplanar coordinated P₄. Besides, the product distribution is sensitive to the presence of coordinated chloride in *meso*-[PtCl-

(9) (a) Scriveri, A.; Camprostrini, R.; Carturan, G. *Inorg. Chim. Acta* **1988**, *142*, 187. (b) Mani, F.; Sacconi, L. *Comments Inorg. Chem.* **1983**, *2*, 166. (c) Brown, M. P.; Fisher, J. R.; Hill, R. H.; Puddephatt, R. J.; Seddon, K. R. *Inorg. Chem.* **1981**, *20*, 3516. (d) Minghetti, G.; Bandini, A. L.; Banditelli, G.; Bonati, F. *J. Organomet. Chem.* **1981**, *214*, C50.

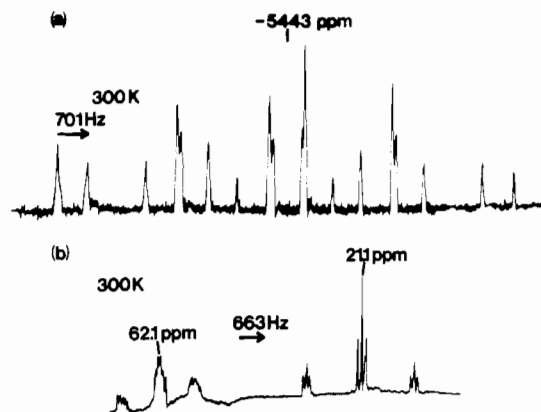
(10) King, R. B.; Kapoor, P. N. *Inorg. Chem.* **1972**, *11*, 1524.

Chart I. Molecular Drawings of Chiral and *meso*-[Pt(P₄)]²⁺, *meso*-[PtCl(P₄)]⁺, and Cations of 1–4^a

^a The P–Pt–P angles where the phosphorus atoms are connected by ethylene chains are constrained to about 85°. As a consequence, the P(1)–Pt–P(3) and P(2)–Pt–(4) angles are about 170° and the P(1)–Pt–P(2) angles about 105° in the square-planar P₄ arrangements (compare ref 7). In 1 and 2 the P(1)–Pt–P(3) and P(2)–Pt–P(4) angles are about 110° and the P(1)–Pt–P(2) angles about 160°, and this coordination is assigned as distorted “tetrahedral” (chiral and *meso*-[PtCl(P₄)](BF₄)) show similar coordinations). In 3 and 4 the coordination is intermediate between square-planar and distorted tetrahedral, the P(1)–Pt–(3) and P(2)–Pt–P(4) angles being about 140° and the P(1)–Pt–P(2) angles about 130°.

(P₄)](BPh₄), leading to a mixture of two compounds of coordination type 2 and 4 instead of the formation of only one product in the case of the reduction of *meso*-[Pt(P₄)](BPh₄)₂. Reduction of *meso*-[PtCl(P₄)](AsF₆) leads to 5, which shows a solvent-dependent equilibrium between the structural types 2 and 4 in solution (see below).

IR Spectra. The infrared spectra of complexes 1–5 show broad strong absorptions above 2000 cm⁻¹, for 1 at 2052 (shoulder) and 2088 cm⁻¹, 2 at 2055 cm⁻¹, 3 and 4 at 2048 cm⁻¹, and 5 at 2055 cm⁻¹. They are in the typical region for Pt–H stretching vibrations of terminal Pt(II) hydrides.^{1b,4a,9c,11} The rather high values of ν(Pt–H) suggest strong Pt–H bonds, in agreement with trans P–Pt–H arrangements.^{1b} The X-ray structure analysis of 3 supports a trans P–Pt–H arrangement, which might be present in the other four complexes as well in the solid state. Interestingly, the Pt–H absorption of 1 consists of two overlapping bands. Since different crystal structures and minor differences in molecular conformation have effects on ν(Pt–H) stretching frequencies,^{9c,11b} this could be a consequence of disorder in the solid state of 1. The corresponding ν(Pt–D) vibrations of 1–5 are not observable and are presumably obscured by Pt–P absorptions. This difficulty has been encountered previously.^{1b,11d} It was not possible to obtain solution IR spectra of complexes 1–5 possibly due to their dynamic solution behavior (see below).

**Figure 1.** (a) Proton-coupled 17.2-MHz ¹⁹⁵Pt NMR spectrum of a CH₂Cl₂ solution of 3. (b) Selectively hydride-coupled 121.5-MHz ³¹P NMR spectrum of a CD₂Cl₂ solution of 4.

NMR Spectra. ¹⁹⁵Pt NMR Spectra. The ¹⁹⁵Pt{¹H} NMR data for 3 and the ³¹P{¹H} NMR parameters for chiral [PtCl(P₄)](BF₄), *meso*-[PtCl(P₄)](BF₄), and for 1–5 are summarized in Table I. The proton-coupled ¹⁹⁵Pt NMR spectrum of 3 is shown in Figure 1a. It consists of 18 lines, consistent with the coupling of the ¹⁹⁵Pt nucleus with two equivalent PPh₂ groups, two equivalent PPh groups, and the hydride ligand. The δ(Pt) value of –5443 for 3 (see Table I) is shifted toward higher field compared with the δ(Pt) values for [PtCl(P₄)]X, where X⁻ = BF₄⁻ and (BPh₄)⁻, and the two diastereomers of [Pt(P₄)](BPh₄)₂ in the range –5084 to –5110.^{6a} A larger shift in the same direction has been observed for the δ(Pt) values for the five-coordinate complexes [PtCl(P–P₃)]Cl and [PtH(PP₃)]Cl of –4372 and –5474, respectively, where PP₃ is tris[2-(diphenylphosphino)ethyl]phosphine and acts as a tetradentate ligand.^{4a} These shifts toward higher fields are a consequence of the high electron-releasing ability of the hydride in contrast to the chloride ligand. The ¹J(Pt,H) value of 701 Hz is comparable to the corresponding value of 755 Hz for [PtH(PP₃)]Cl. Though strongly dependent on the coordination properties, the difference of the two values can be explained by the small trans influence of a phosphino group relative to a hydride ligand,^{11a,12} increasing ¹J(Pt,H) in [PtH(PP₃)]Cl. In contrast to [PtH(PP₃)]Cl the dynamic solution structure of 3 contains no measurable trans P–Pt–H arrangement (see below), thus decreasing ¹J(Pt,H) in 3. Due to their lower solubilities no ¹⁹⁵Pt NMR spectra for 1, 2, 4, and 5 could be obtained.

³¹P{¹H} NMR Spectra of Distorted “Tetrahedral” Complexes. The 121.5-MHz ³¹P{¹H} NMR spectra of chiral [PtCl(P₄)](BF₄) and *meso*-[PtCl(P₄)](BF₄) show three well-resolved broad peaks all containing ¹⁹⁵Pt satellites consistent with AB₂C spin systems and distorted tetrahedral arrangements of P₄.^{6a} Similar 121.5-MHz ³¹P{¹H} NMR spectra were obtained for 1 and 2, showing two well-resolved broad peaks together with ¹⁹⁵Pt satellites consistent with A₂B₂ spin systems and also with tetrahedral arrangements of P₄. The spectra are temperature dependent, and the two peaks coalesce to one broad peak at about 245 K with δ(P) = 34.7 and ¹J(Pt,P) = 1990 Hz for 1 and 2. In none of the complexes containing tetrahedral P₄ were ²J(PPh,PPh₂) couplings resolved, indicating the presence of substantial imbalances in tetrahedral P₄ coordination populations.¹³ The δ(P) values of 1 and 2 are shifted toward higher fields compared with the corresponding values of the two diastereomers of [PtCl(P₄)](BF₄). The ¹J(Pt,P) parameters are smaller in 1 and 2 than in chiral and *meso*-[PtCl(P₄)](BF₄) (compare Table I). In all complexes containing tetrahedral P₄ assignment of the PPh and PPh₂ groups of P₄ in the 121.5-MHz ³¹P{¹H} NMR spectra is difficult.^{6a} However, it seems likely that the low-field signals in 1 and 2 correspond to the PPh groups being part of two chelating five-

(11) (a) Tau, K. D.; Meek, D. W. *Inorg. Chem.* **1979**, *18*, 3574. (b) Brown, M. P.; Fisher, J. R.; Manojlović-Muir, L.; Muir, K. W.; Puddephatt, R. J.; Thomson, M. A.; Seddon, K. R. *J. Chem. Soc., Chem. Commun.* **1979**, 931. (c) Barker, G. K.; Green, M.; Onak, T. P.; Stone, F. G. A.; Ungermann, Ch. B.; Welch, A. J. *J. Chem. Soc., Chem. Commun.* **1978**, 169. (d) Minghetti, G.; Banditelli, G.; Bandini, A. L. *J. Organomet. Chem.* **1977**, *139*, C80. (e) Furnies, J.; Green, M.; Spencer, J. L.; Stone, F. G. A. *J. Chem. Soc., Dalton Trans.* **1977**, 1006.

(12) (a) Brüggeller, P. *Inorg. Chem.* **1987**, *26*, 4125. (b) Hohman, W. H.; Koutz, D. J.; Meek, D. W. *Inorg. Chem.* **1986**, *25*, 616.

(13) Bookham, J. L.; McFarlane, W.; Colquhoun, I. J. *J. Chem. Soc., Chem. Commun.* **1986**, 1041.

membered rings instead of only one in the case of the PPh₂ groups,^{6a,14} which are attributed to the high-field signals.

³¹P{¹H} NMR Spectra of 3 and 4. On the basis of the above argument, the PPh and PPh₂ groups are easily assigned in 3 and 4 since their ³¹P{¹H} NMR spectra are consistent with A₂M₂ spin systems. The δ(PPh) and δ(PPh₂) values for 3 and 4 are shifted toward higher fields compared with the corresponding values for *meso*-[PtCl(P₄)](BPh₄) and the two diastereomers of [Pt(P₄)]-(BPh₄)₂ (Table 1^{6a}). This is the same trend as already mentioned for the complexes containing tetrahedral P₄. However, in contrast to *meso*-[PtCl(P₄)](BPh₄), chiral [Pt(P₄)](BPh₄)₂, and *meso*-[Pt(P₄)](BPh₄)₂, the ³¹P{¹H} NMR spectra of these compounds showing two doublets (²J_{cis}(PPh,PPh₂) + ³J(PPh,PPh₂) is zero), the arrangement of P₄ is no longer square-planar in 3 and 4. Both ³¹P{¹H} NMR signals of the A₂M₂ spin systems are split into triplets, where ²J(PPh,PPh₂) + ³J(PPh,PPh₂) is 80 and 82 Hz for 3 and 4. Values of ²J_{cis}(P,P) for platinum(II) complexes fall in the range 10–50 Hz, while values of ²J_{trans}(P,P) are typically 1 order of magnitude larger.^{1d,3a,6a,9c,11a,12a,15} The corresponding values for 3 and 4 are located between the ²J_{cis}(P,P) and ²J_{trans}(P,P) ranges. An arrangement of P₄, in which the two pairs of PPh and PPh₂ groups, respectively, include two angles between 110 and 170°, is obtained if P₄ moves along the reaction coordinate from a square-planar toward a tetrahedral arrangement.^{8b} Thus, the coordination of P₄ is intermediate between a square-planar and a tetrahedral geometry in 3 and 4. If the hydride ligand in 3 and 4 is included, this means that one pair of the two pairs of PPh and PPh₂ groups, respectively, is bent toward, the other away from, the hydride ligand resulting in cisoid and transoid arrangements.

Selectively Hydride-Coupled ³¹P NMR Spectra of 3 and 4. Figure 1b shows a selectively proton-coupled 121.5-MHz ³¹P NMR spectrum of 4, which reveals the splitting of the PPh resonance into a doublet by ²J(PPh,H) of about 80 Hz. Selective hydride couplings are only resolved if the P–H coupling constants involved are large enough.^{1d,4a,16} Typical ²J_{cis}(P,H) values are <25 Hz and ²J_{trans}(P,H) values >100 Hz.^{1c,9a,c,d,11a,c,e,14b} However, intermediate values of about 40 Hz have been found for (μ-H)₂^{1b,17} and (μ-H) structures.¹⁸ In the latter case it has been shown that the intermediate values are due to fluxionality and are resolved into two coupling values of about 80 and 10 Hz at the rigid limit. Regarding their magnitude and in view of the known X-ray structure of a corresponding (μ-H) compound,¹⁸ the two coupling values are best described as transoid and cisoid ²J(P,H) couplings, respectively. In 3 and 4 the selectively hydride-coupled ³¹P resonances of the PPh groups are split by ²J_{transoid}(PPh,H) of about 80 Hz; the splitting of the PPh₂ groups by ²J_{cisoid}(PPh₂,H) is not resolved (see below). The coordination of the hydride ligand transoid to the PPh and cisoid to the PPh₂ groups, respectively, is confirmed by the ¹J(Pt,PPh) and ¹J(Pt,PPh₂) values. The ¹J(Pt,PPh) values for 3 and 4 are smaller and the ¹J(Pt,PPh₂) values are larger than the corresponding values for *meso*-[PtCl(P₄)](BPh₄), chiral [Pt(P₄)](BPh₄)₂, and *meso*-[Pt(P₄)]-(BPh₄)₂ (Table 1^{6a}). This is in agreement with the observed trans and cis influence for the hydride ligand^{11a,12a} and is shown to be reliable for transoid and cisoid influences as well. The ³¹P{¹H} NMR signals for 3 and 4 are temperature dependent and are broadened on cooling. At about 245 K coupling due to ²J(PPh,PPh₂) is completely lost, indicating now substantial imbalances in P₄ coordination populations. This shows that at room temperature the fast-exchange limit for the dynamic intramo-

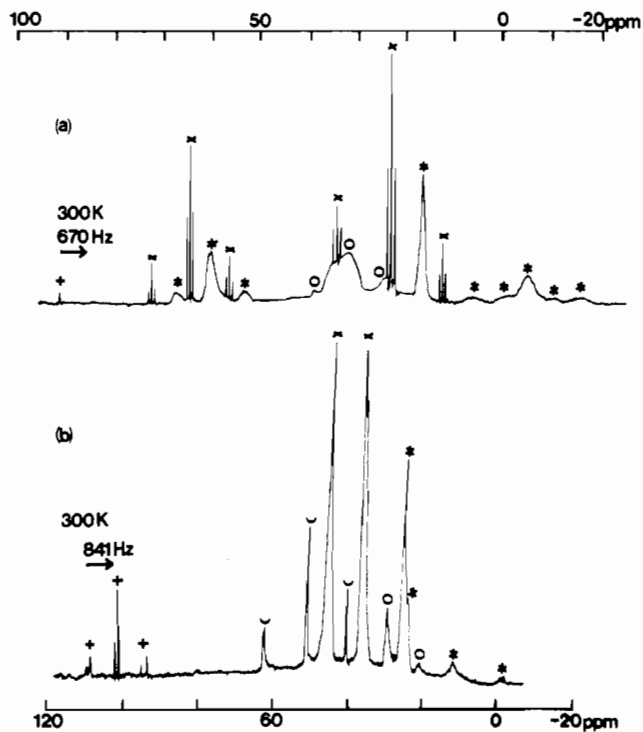


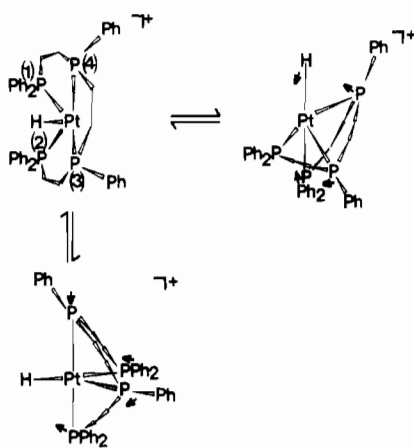
Figure 2. (a) 121.5-MHz ³¹P{¹H} NMR spectrum of a CD₃NO₂ solution of 5. The labeling on the spectrum corresponds to the following sets of signals: (O) structural type 2; (X) structural type 4; (*) intermediate; (+) apical position (Berry process). (b) Selectively hydride-coupled 121.5-MHz ³¹P NMR spectrum of an acetone-*d*₆ solution of 5. The labeling on the spectrum corresponds to the following sets of signals: (O) structural type 2; (X) flattened version of structural type 4; (*) intermediate; (+) apical position (Berry process); (U) equatorial position (Berry process).

lecular process is reached.¹⁹ At this temperature rapid phosphine site-exchange leads to averaging of the P₄ coordination, resulting in the resolution of ²J(PPh,PPh₂). A similar dynamic behavior has been observed for several hydrido-bridged platinum(II) species.^{1b–e,16,20}

³¹P{¹H} NMR Spectra of a CD₃NO₂ Solution of 5. Figure 2a shows the ³¹P{¹H} NMR spectrum of a CD₃NO₂ solution of 5. It contains the spectral patterns typical for coordination types 2 and 4 (compare Table I) and three further sets of signals due to the dynamic nature of the transformation of structural types 2 and 4 along the tetrahedral to square-planar reaction coordinate. Since the hydride ligand in 2 shows “tetrahedral jumping”²¹ (see below), the three sets of signals belong to structural type 4, accounting for the necessity of significant variations in metal–ligand interaction due to the transition from a localized hydride ligand in 4 to a delocalized ligand in 2.^{21,22} In this intermediate the PPh groups located transoid to the hydride ligand in 4 are only slightly influenced, leading to a broad signal with δ = 60.2 containing ¹⁹⁵Pt satellites (¹J(Pt,P) = 1695 Hz). It corresponds to imbalanced PPh groups showing a smaller coupling to ¹⁹⁵Pt than in 4 (1695 vs 1992 Hz) due to their movement along the square-planar to tetrahedral reaction coordinate in contrast to the PPh groups in 4 being in the fast-exchange limit. In the intermediate the deviation of the PPh₂ groups from their fast-exchange limit structure in 4 is larger due to their coordination cisoid to the hydride ligand in 4.²¹ Two sets of signals are attributed to the PPh₂ groups. The broad peak containing no ¹⁹⁵Pt satellites with δ = 16.6 similar to

(14) Garrou, P. E. *Chem. Rev.* **1981**, *81*, 229.
 (15) (a) DuBois, D. L.; Miedaner, A. J. *Am. Chem. Soc.* **1987**, *109*, 113. (b) Brown, M. P.; Fisher, J. R.; Mills, A. J.; Puddephatt, R. J.; Thomson, M. *Inorg. Chim. Acta* **1980**, *44*, L271.
 (16) (a) Lemmen, T. H.; Lundquist, E. G.; Rhodes, L. F.; Sutherland, B. R.; Westerberg, D. E.; Caulton, K. G. *Inorg. Chem.* **1986**, *25*, 3915. (b) Bracher, G.; Grove, D. M.; Pregosin, P. S.; Venanzi, L. M. *Angew. Chem.* **1979**, *91*, 169.
 (17) Tulip, T. H.; Yamagata, T.; Yoshida, T.; Wilson, R. D.; Ibers, J. A.; Otsuka, S. *Inorg. Chem.* **1979**, *18*, 2239.
 (18) Minghetti, G.; Bandini, A. L.; Banditelli, G.; Bonati, F.; Szostak, R.; Strouse, C. E.; Knobler, C. B.; Kaesz, H. D. *Inorg. Chem.* **1983**, *22*, 2332.

(19) Harris, R. K. *Nuclear Magnetic Resonance Spectroscopy*; Longman Scientific & Technical: Avon, U.K., 1986; p 121.
 (20) Brown, M. P.; Puddephatt, R. J.; Rashidi, M.; Seddon, K. R. *J. Chem. Soc., Dalton Trans.* **1978**, 516.
 (21) Meakin, P.; Muettterties, E. L.; Jesson, J. P. *J. Am. Chem. Soc.* **1972**, *94*, 5271.
 (22) English, A. D.; Meakin, P.; Jesson, J. P. *J. Am. Chem. Soc.* **1976**, *98*, 422.

Scheme I^a

^a The involvement of **4** in a Berry-type rearrangement process leads to two trigonal bipyramids, which are distorted as a consequence of the electronic forces to form ideal trigonal bipyramids and the steric requirements of *meso*-P₄.²⁸ The coordination with the hydride ligand in one axial position is the energetically favored trigonal bipyramid.

$\delta = 23.3$ of the PPh₂ groups in the fast-exchange limit is indicative of a retained but decreased Pt–P interaction^{3a} in a position comparable to the PPh₂ coordination in **4**. The second broad signal occurs at higher field ($\delta = -5.5$), showing ¹⁹⁵Pt satellites ($^1J(\text{Pt}, \text{PPh}_2) = 2693$ Hz). The appearance of a second set of satellites ($^1J(\text{Pt}, \text{PPh}_2) = 1214$ Hz) indicates the presence of a further peak hidden by the signal at -5.5 ppm. Both peaks are shifted toward the resonance of free PPh₂ groups at about -12 ppm and correspond to dissociatively unstable Pt–P bonds, resulting in nearly dangling PPh₂ positions.^{12a,23} This is confirmed by the large difference of the above $^1J(\text{Pt}, \text{PPh}_2)$ values. Both signals account for substantial imbalances in these dissociatively unstable Pt–PPh₂ populations.

Temperature Dependence of the ³¹P{¹H} NMR Spectra of the Intermediate. All resonances of the intermediate are temperature dependent. At 283 K the partly hidden PPh₂ peak now at about -4.2 ppm is split into a triplet clearly seen in its corresponding ¹⁹⁵Pt satellites with $^1J(\text{Pt}, \text{PPh}_2) = 1468$ and $^2J(\text{PPh}, \text{PPh}_2) = 164$ Hz, the PPh signal showing the same triplet and $^2J(\text{PPh}, \text{PPh}_2)$ value. The split PPh₂ signal corresponds to a balanced PPh₂ coordination population at this temperature, the $^2J(\text{PPh}, \text{PPh}_2)$ value being two times larger than the corresponding value in **4** but still smaller than typical $^2J_{\text{trans}}(\text{P}, \text{P})$ couplings.^{11a,12a,15a} This is explained by the movement of the P₄ coordinates toward a square-planar coordination thus opening the angles between the two pairs of PPh and PPh₂ groups, respectively. On further cooling, the above coupling disappears again and at 247 K the signals corresponding to dissociatively unstable Pt–PPh₂ groups are very broad and centered at about -3.0 ppm ($^1J(\text{Pt}, \text{PPh}_2) = 2854$ and 1263 Hz). At this temperature also the other two sets of signals assigned to the intermediate are very broad. This indicates that the P₄ coordination populations are now substantially imbalanced again.

Furthermore, the ³¹P{¹H} NMR spectra of a CD₃NO₂ solution of **5** show a weak low-field peak with $\delta = 91.9$ already at 300 K. On cooling, this signal intensifies and at 283 K coupling to ¹⁹⁵Pt is resolved ($\delta = 92.8$, $^1J(\text{Pt}, \text{P}) = 2280$ Hz). Though for five-coordinate molecules containing pseudotetrahedral substructures the “tetrahedral jump” mechanism has been favored²² and accounts for the above described dynamic behavior of CD₃NO₂ solutions of **5**, the presence of a second mechanism, the Berry pseudorotation,²⁴ cannot be ruled out.^{3c,17,21}

The Berry Mechanism in **5.** Since the Berry mechanism is strictly applicable only to trigonal-bipyramidal XML₄ species of

C_{2v} symmetry, a transition state distinct from a square pyramid may result if the trigonal bipyramid is distorted. A possible Berry-type mechanism for structural type **4** leading to distorted trigonal bipyramids is shown in Scheme I. Since the chelate terminal arms of *meso*-P₄ are constrained to move toward the same apical position if the PPh groups occupy two equatorial sites of a trigonal bipyramid, this invariably leads to an apical coordination of the hydride ligand.^{6d} Similarly, if a PPh group occupies an apical position, the PPh₂ groups are forced to move toward the same equatorial position and only a trigonal-bipyramidal arrangement is possible in which the hydride ligand occupies an equatorial position. Since trigonal bipyramids with the hydride ligand in an equatorial position are much less stable than those with the hydrogen axial,^{21,25} the apical coordination of a PPh₂ group is assumed. This is confirmed by the large downfield shift of the above signal typical for a phosphorus atom trans to a hydride ligand^{12a} and by comparison with the dynamic behavior of an acetone-*d*₆ solution of **5** (see below). However, the easy exchange of axial and equatorial coordination sites typical for a Berry-type mechanism also includes the two PPh and PPh₂ groups of P₄ analogous to Scheme I, thus leading to an exchange of the terminal PPh₂ groups in their apical positions trans to the hydride ligand.

Selectively Hydride-Coupled ³¹P NMR Spectra of an Acetone-*d*₆ Solution of **5.** Figure 2b shows a selectively hydride-coupled ³¹P NMR spectrum of an acetone-*d*₆ solution of **5**. The signal at 28.6 ppm ($^1J(\text{Pt}, \text{P}) = 2016$ Hz) is attributed to structural type **2** (compare Table I), the broad peak with $\delta 24.3$ containing no ¹⁹⁵Pt satellites to imbalanced PPh₂ groups of structural type **4**, and the weak signal at 11.3 ppm ($^1J(\text{Pt}, \text{PPh}_2) = 2892$ Hz) to dissociatively unstable PPh₂ groups. The latter two sets of peaks correspond to the presence of the tetrahedral jump mechanism as described above. The two signals assigned to the PPh and PPh₂ groups (compare Table I) are shifted toward higher and lower fields, respectively, when compared with the corresponding values of **4**, and the difference between the two values of 41 ppm in **4** diminishes to about 9 ppm in an acetone-*d*₆ solution of **5**. In this solution both signals are broad triplets with a $^2J(\text{PPh}, \text{PPh}_2)$ value of 46 Hz containing no ¹⁹⁵Pt satellites. This is indicative for a retained but decreased Pt–P interaction in a flattened version of structural type **4** showing imbalances in its P₄ coordination populations and is confirmed by the small $^2J(\text{PPh}, \text{PPh}_2)$ value now in the cisoid range, reflecting a smaller angle between the two pairs of PPh and PPh₂ groups, respectively. Both peaks show further, however not completely resolved, splitting due to $^2J(\text{P}, \text{H})$ of about 24 Hz also in the cisoid range. The flattened version of structural type **4** is in better agreement with the required square-pyramidal transition state for an idealized Berry mechanism analogous to Scheme I.²¹

The further two sets of signals in Figure 2b indicate that the Berry mechanism is the dominant rearrangement mechanism in acetone-*d*₆ solutions of **5**. The peaks at 50.6 ($^1J(\text{Pt}, \text{P}) = 2608$ Hz) and 101.8 ppm ($^1J(\text{Pt}, \text{P}) = 1859$ Hz) are assigned to the equatorial and apical phosphorus atoms of a trigonal bipyramid (compare Table I and Chart I) and correspond to balanced P₄ coordination sites presumably in the fast-exchange limit. Both signals show a splitting into doublets due to $^2J(\text{P}_{\text{eq}}, \text{P}_{\text{ap}})$ of 34 Hz in the cisoid range, the P_{eq} peak being further split by $^2J_{\text{cis}}(\text{P}_{\text{eq}}, \text{H})$ of about 2 Hz (not well resolved) and the P_{ap} peak by $^2J_{\text{trans}}(\text{P}_{\text{ap}}, \text{H})$ of 128 Hz. These splittings indicate the presence of an axial hydride ligand, leading to the occupation of the second axial position of the trigonal bipyramid by a PPh₂ group (compare Scheme I). This is confirmed by the large difference in the above $^1J(\text{Pt}, \text{P})$ values typical for five-coordinate platinum(II) hydrides with the hydride ligand in one axial position,^{12a,22,25} reflecting a strong trans and a weak cis influence of the hydride ligand.^{11a} However, since the occurrence of only one very sharp equatorial signal accounts for the fact that the P_{eq} and P_{ap} signals are in the fast-exchange limit according to Scheme I, the two terminal PPh₂ groups are interchanged in their apical positions as described

(23) Tau, K. D.; Uriarte, R.; Mazanec, T. J.; Meek, D. W. *J. Am. Chem. Soc.* **1979**, *101*, 6614.
(24) Berry, R. S. *J. Chem. Phys.* **1960**, *32*, 933.

(25) Ebsworth, E. A. V.; Edward, J. M.; Reed, F. J. S.; Whitelock, J. D. *J. Chem. Soc., Dalton Trans.* **1978**, 1161.

Table II. ^1H NMR Data for the Hydride Region of 1–5^{a,c}

compd	$\delta(\text{H})$	$^1J(\text{Pt-H})$	$^2J_{\text{cisoid}}(\text{P,H})$	$^2J_{\text{transoid}}(\text{P,H})$
1	-9.7 (q) ^b	nr ^e	9	
2	-9.6 (q) ^b	nr ^e	10	
3	-9.7 (tt) ^a	701	13	78
4	-9.8 (tt) ^a	701	14	79
5a	-9.7 (tt) ^a	713	13	78
5b	-9.7 (q) ^b	nr ^e	9	
5b	-10.8 (qq) ^d	1242	2 (cis)	126 (trans)

^a J values in Hz. Spectra were run at 303 K. ^bSpectra were obtained at 253 K. ^c1, 2, and 5a were measured in CD_3NO_2 , 3 and 4 were measured in CD_2Cl_2 , and 5b was measured in acetone- d_6 ; all spectra were run at 300 MHz; q = quintet, tt = triplet of triplets, and qq = quintet of quintets. ^dThe spectrum was obtained at 312 K. ^enr = not resolved.

above. In fact, a rotation-like mechanism could result, in which P_4 moves around a platinum(II) center like the chain of a bicycle, the hydride ligand in axial position being the dominant coordination population within the different trigonal-bipyramidal stereoisomers. All signals of Figure 2b are only slightly influenced by temperature variations in the experimentally feasible region from 315 to 253 K. This confirms the presence of a very fast rearrangement mechanism in acetone- d_6 solutions of 5.

^1H NMR Spectra. The 300-MHz ^1H NMR spectra of complexes 1–5 show three different regions of signals corresponding to the phenyl protons, the ethylene protons, and the hydride ligands. The ^1H NMR signals of the phenyl groups in 1 and 2 are broad unresolved peaks at about 7.5 ppm at 303 K and further broaden on cooling. The signals of the ethylene protons centered at about 2.5 ppm show a similar behavior but are too strongly broadened to be observable at about 243 K. Both sets of peaks indicate the presence of substantial imbalances in tetrahedral P_4 coordination populations, as described above. In 3 and 4 two phenyl rings show well-resolved ^1H NMR signals consisting of five peaks in the range 7.18–7.28 ppm and five peaks in the range 7.33–7.41 ppm. These signals are attributed to the PPh groups. The peaks corresponding to the PPh_2 groups coincide and show a broad signal centered at 7.43 ppm containing several shoulders (the intensity ratio of the signals assigned to the PPh and PPh_2 groups, respectively, is 1:2). The phenyl ring ^1H NMR signals for 3 and 4 account for the fact that both complexes are in the fast-exchange limit at room temperature. As a consequence, the above resolution of different phenyl ring signals is lost on cooling and at 243 K only one broad peak centered at 7.5 ppm is observed. The ethylene protons in 3 and 4, respectively, show a broad signal centered at 2.5 ppm, which further broadens on cooling and is unobservable at about 243 K. This indicates imbalanced ethylene groups in 3 and 4 already at room temperature and a different dynamic behavior of the bridging ethylene groups of the two molecules, which has been observed for other polyphosphine complexes as well.²⁶ Besides the signals according to structural types 2 and 4 mentioned above, CD_3NO_2 solutions of 5 contain two sets of two broad peaks at 6.97 and 7.07 ppm and at 5.99 and 6.15 ppm, respectively, in intensity ratio 2:1, assigned to the phenyl rings of the PPh_2 and PPh groups, and two broad signals at 1.58 and 1.87 ppm corresponding to the ethylene groups of the intermediate. Both sets of signals broaden on cooling, the ethylene signals being undetectable at about 243 K. Acetone- d_6 solutions of 5 show a broad unresolved peak at 7.45 ppm containing a shoulder at 7.70 ppm assigned to the phenyl rings and no ethylene signal already at 303 K. This accounts for the fast Berry-type rearrangement in acetone- d_6 solutions of 5, as described above.

In Table II the 300-MHz ^1H NMR data of the hydride regions for complexes 1–5 are summarized. Hydride chemical shifts are known to be particularly sensitive to the nature of trans ligands and different coordination geometries and cover a shift range of about 25 ppm.^{1b-d,4a,9a,c,11a,16a,17,20} The δ values of Table II are located within the central region of this shift range. The hydride resonance of acetone- d_6 solutions of 5 is shifted toward higher

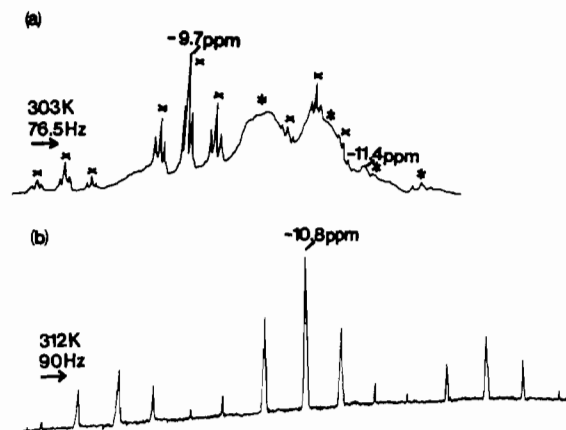


Figure 3. (a) 300-MHz ^1H NMR spectrum of the hydride region of a CD_3NO_2 solution of 5. The labeling on the spectrum corresponds to the following sets of signals (structural type 2 is hidden by the signal at -9.7 ppm): (X) structural type 4, (*) intermediates. (b) 300-MHz ^1H NMR spectrum of the hydride region of an acetone- d_6 solution of 5. The signals correspond to the fast-exchange limit of the Berry process.

field compared with those of CD_3NO_2 and CD_2Cl_2 solutions, respectively, of complexes 1–5. This is explained by the weak trans influence of a phosphino group relative to the hydride ligand, a trans P–Pt–H arrangement in large amount being only present in acetone- d_6 solutions of 5.^{1c} A similar trend is observed in the $^1J(\text{Pt,H})$ values located in the typical range for terminal hydrides^{1b,c,9a,c,11a,15b,25} being larger in 5 than in 3 and 4 and strongly increasing with growing amount of trans P–Pt–H arrangement present. The ^1H NMR spectra of the hydride region of 1 and 2 are broad unresolved peaks at 303 K indicating that the tetrahedral jump mechanism described above is fast on the NMR time scale at this temperature. At 253 K a quintet is resolved with $^2J_{\text{cisoid}}(\text{P,H})$ of about 10 Hz located in the range typical for $^2J_{\text{cis}}(\text{P,H})$ values (see above). This corresponds to coupling of the hydride ligand with four equivalent phosphorus atoms in the fast-exchange limit in agreement with the favored tetrahedral jump mechanism showing the lowest energy path for hydrogen migration and the hydride ligand capping the tetrahedral faces.²¹ At lower temperatures this coupling is lost again, accounting for the now dominating imbalances in P_4 coordination populations. The ^1H NMR spectra of the hydride region of 3 and 4 consist of triplets of triplets containing ^{195}Pt satellites at 303 K produced by cisoid and transoid couplings of two equivalent PPh and PPh_2 groups, respectively, and the ^{195}Pt nucleus with the hydride ligand (compare Table II). The full resolution of these couplings corresponds to the fast-exchange limits of solution structures 3 and 4 at this temperature, as described above. On cooling, all peaks broaden and at 253 K $^2J_{\text{cisoid}}(\text{PPh}_2,\text{H})$ is unresolved. At 243 K coupling is completely lost and only a very broad peak centered at -9.7 ppm remains. This temperature behavior confirms the already reported occurrence of substantial imbalances in P_4 coordination populations on cooling solutions of 3 and 4.

Figure 3a shows the 300-MHz ^1H NMR spectrum of the hydride region of a CD_3NO_2 solution of 5. Besides the peaks characteristic for structural type 4 (compare Table II), where the broad peak at -9.7 ppm corresponding to structural type 2 is hidden by the central peak of structural type 4 at 303 K, Figure 3a contains two broad peaks at -10.41 and -10.87 ppm, respectively, and a broad triplet of triplets centered at -11.4 ppm with $^2J_{\text{cisoid}}(\text{PPh}_2,\text{H})$ of 27 Hz and $^2J_{\text{transoid}}(\text{PPh},\text{H})$ of 169 Hz. The low-field triplet of the latter set of signals is partly hidden by other peaks, and no ^{195}Pt satellites are resolved. Both sets of signals are attributed to the transition from a localized hydride ligand in structural type 4 to a delocalized ligand in structural type 2. The broad triplet of triplets corresponds to the imbalanced version of structural type 4 as observed in the $^{31}\text{P}\{^1\text{H}\}$ NMR spectra of CD_3NO_2 solutions of 5 (see above). The larger $^2J(\text{P,H})$ values compared with the corresponding values in 4 (Table II) confirm the movement of the imbalanced intermediate along the square-planar to tetrahedral reaction coordinate, thus opening the

PhP–Pt–H and Ph₂P–Pt–H angles and increasing both ²J(P,H) values. The opening of the Ph₂P–Pt–H angle is certainly a consequence of the presence of dissociatively unstable Pt–PPh₂ coordination populations in the intermediate, as indicated by the ³¹P{¹H} NMR spectra of **5** (see above). The two broad peaks in Figure 3a are assigned to different modes of the tetrahedral jump mechanism, being fast on the NMR time scale and indicative for the transition from a localized hydride ligand in structure type **4** to a delocalized in structural type **2**. Both sets of signals are temperature dependent. The broad triplet of triplets broadens further on cooling and the ²J(PPh₂,H) value increases to 72 Hz at 283 K, indicating a further opening of the PPh₂–Pt–H angle and presumably corresponding to the balanced Pt–PPh₂ coordination population at this temperature (see above). At lower temperatures this signal is not further observable due to the now occurring substantial imbalances in P₄ coordination populations. The two broad peaks in Figure 3a coincide to one broad peak with δ = –10.6 at 263 K, which is shifted to δ = –10.4 at 253 K and is unobservable at about 245 K. This indicates that in these intermediate modes of the tetrahedral jump mechanism the imbalances in P₄ coordination populations lead to a disappearance of the signals on cooling before the slow-exchange limit is reached.

Figure 3b shows the 300-MHz ¹H NMR spectrum of the hydride region of an acetone-*d*₆ solution of **5**. It consists of a quintet produced by four equivalent phosphorus atoms in the fast-exchange limit (compare Table II). This corresponds to the fast Berry-type rearrangement resulting in a P₄ rotation-like mechanism observed in the ³¹P{¹H} NMR spectra of an acetone-*d*₆ solution of **5**, as described above. Since the hydride ligand in an axial position of a trigonal bipyramid is the dominant coordination population, the above coupling results upon rotation-like movement of P₄ in the fast-exchange limit. The ²J(P,H) value of 126 Hz is located within the range typical for a ²J_{trans}(P,H) coupling (see above) in agreement with the trigonal-bipyramidal coordination and occurring also in the already mentioned selectively hydride coupled ³¹P NMR spectra of an acetone-*d*₆ solution of **5**. However, since the above dynamic process decreases T₁ of the ¹H nucleus, spin excitation problems have occurred during ¹H NMR measurement being typically larger at higher fields.²⁷ At lower temperatures the signal is shifted to higher fields and centered at –13.3 ppm at 303 K. The ²J_{trans}(P,H) coupling is now 128 Hz. However, the multiplicity has changed; 28 peaks are observed as a whole, and except for the central lines, it is difficult to distinguish between main peaks and ¹⁹⁵Pt satellites as a consequence of spin excitation problems. Each line is split into a triplet by a ²J_{cis}(P,H) coupling of about 2 Hz. This indicates that the above trigonal-bipyramidal coordination with the hydride ligand in axial position remains the dominating coordination population. The higher multiplicity is assigned to a slower P₄ movement within the rotation-like rearrangement process, resulting in individual trans coupling of each phosphorus atom and the resolution of a cis coupling of only one pair of the two pairs of PPh and PPh₂ groups, respectively, present. Including ¹⁹⁵Pt satellites, this could lead to 48 triplets of which only 28 are observed. At 273 K a further splitting due to ²J_{cisoid}(P,H) of about 24 Hz occurs corresponding to the now feasible presence of the flattened version of structural type **4** as the Berry-type intermediate in the rotation-like rearrangement process. This coupling has also been observed in the selectively hydride-coupled ³¹P NMR spectra of acetone-*d*₆ solutions of **5**, as mentioned above. Only slight changes in spectral parameters occurred on further cooling.

X-ray Crystal Structure of Chiral [PtH(P₄)](BPh₄) (3**).** Figure 4 shows the molecular structure of the cation of **3**.²⁸ Fractional atomic coordinates and isotropic thermal parameters of **3** are given in Table III. Table IV contains the crystallographic data for **3**. The relation between the solution structure of **3** as discussed above and its solid-state structure is shown in Scheme II. The solution structure of **3** corresponds to the intermediate in a possible

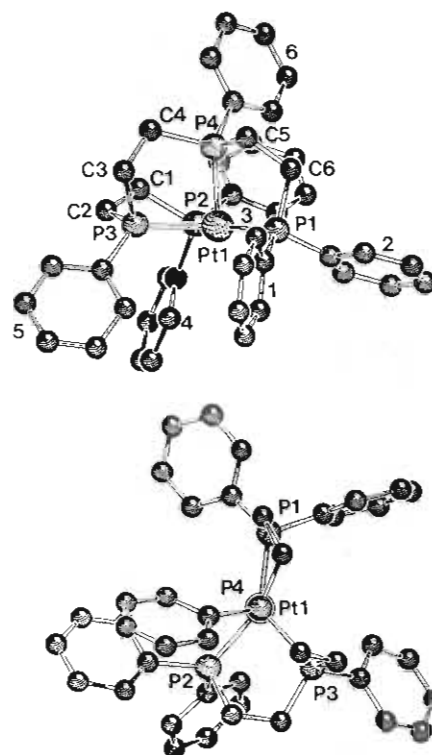
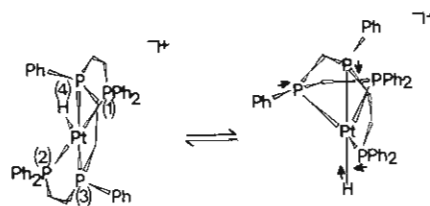


Figure 4. Structure of the cation of **3**: (a) Pt(1)–P(4) bond in the projection plane; (b) projection along the P(4)–Pt(1) bond. Selected bond distances (Å) and angles (deg) (standard deviations are given in form of the last significant figure in parentheses): Pt(1)–P(1) = 2.239 (5), Pt(1)–P(2) = 2.346 (4), Pt(1)–P(3) = 2.342 (6), Pt(1)–P(4) = 2.286 (4); P(1)–Pt(1)–P(2) = 145.6 (2), P(2)–Pt(1)–P(3) = 84.9 (2), P(3)–Pt(1)–P(1) = 129.5 (2), P(1)–Pt(1)–P(4) = 86.9 (2), P(2)–Pt(1)–P(4) = 99.5 (2), P(3)–Pt(1)–P(4) = 84.0 (2). The platinum atom is shifted out of the equatorial plane by 0.015 Å toward the hydride ligand.

Scheme II^a



^a A Berry-type rearrangement in **3** leads to a trigonal bipyramid with the hydride ligand in one axial position as the energetically favored coordination, which is strongly distorted due to the electronic forces to form an ideal trigonal bipyramid and the steric requirements of chiral P₄.²⁸ This coordination corresponds to the solid-state structure of **3**.

Berry-type rearrangement according to Scheme II leading to a trigonal bipyramid with the hydride ligand in an axial position as the energetically favored coordination geometry within the trigonal-bipyramidal coordinations analogous to Scheme I (see above). Since **3** contains chiral P₄, the hydride ligand in axial position leads to a PPh group in the other axial position of the trigonal bipyramid for reasons explained above. This is the coordination geometry of the solid-state structure of **3** seen in Figure 4. A deviation of solution structures from the corresponding solid-state structures is typical for molecules showing fluxional behavior in solution, and the low-temperature solution form is often expected to be the same as the solid-state structure.^{1a-c,4d} If a Berry mechanism is involved, the static-limit structure is a trigonal bipyramid corresponding to that in Scheme II.^{17,21} Though no direct evidence of a Berry mechanism was obtained in CH₂Cl₂ solutions of **3**, the solution behavior of **5** strongly suggests that this mechanism is present in a small amount in solutions of **3** as well, thus leading to the observed solid-state structure of **3**. The trigonal-bipyramidal coordination of **3** is strongly distorted (Figure

(27) Faller, J. W. In *Determination of Organic Structures by Physical Methods*; Nachod, F. C., Zuckerman, J. J., Eds.; Academic Press: New York, 1973.

Table III. Fractional Atomic Coordinates and Thermal Parameters of Non-Hydrogen Atoms^a

atom	<i>x/a</i>	<i>y/b</i>	<i>z/c</i>	<i>B</i> _{eq} , Å ²	atom	<i>x/a</i>	<i>y/b</i>	<i>z/c</i>	<i>B</i> _{eq} , Å ²
Pt(1)	0.1125 (1)	0.2518 (05)	0.3600 (05)	2.8 (02)	C(52)	-0.0916 (19)	0.2171 (17)	0.1499 (15)	8.5 (15)
P(1)	0.0339 (4)	0.2524 (3)	0.4984 (3)	4.2 (2)	C(53)	-0.1378 (27)	0.1564 (25)	0.1339 (23)	13.1 (25)
P(2)	0.2894 (4)	0.2323 (3)	0.2586 (3)	3.5 (2)	C(54)	-0.1614 (29)	0.0927 (21)	0.1998 (25)	11.6 (23)
P(3)	0.0173 (4)	0.2730 (3)	0.2437 (3)	3.9 (2)	C(55)	-0.1248 (29)	0.0756 (17)	0.2800 (25)	15.0 (25)
P(4)	0.0374 (4)	0.4062 (3)	0.3379 (3)	3.6 (2)	C(56)	-0.0747 (20)	0.1349 (14)	0.2999 (17)	8.9 (15)
C(1)	0.2349 (14)	0.3056 (12)	0.1581 (10)	4.8 (9)	C(61)	0.1349 (15)	0.4721 (11)	0.3186 (11)	3.8 (9)
C(2)	0.1287 (16)	0.2845 (12)	0.1458 (10)	5.4 (10)	C(62)	0.1125 (16)	0.5560 (12)	0.2623 (11)	5.2 (10)
C(3)	-0.1021 (14)	0.3857 (10)	0.2365 (11)	4.5 (9)	C(63)	0.1927 (21)	0.6047 (13)	0.2465 (13)	6.3 (12)
C(4)	-0.0514 (15)	0.4538 (10)	0.2464 (11)	4.4 (9)	C(64)	0.2915 (20)	0.5704 (15)	0.2898 (15)	6.6 (13)
C(5)	-0.0721 (15)	0.4361 (10)	0.4333 (11)	4.1 (9)	C(65)	0.3125 (17)	0.4892 (15)	0.3478 (14)	6.7 (12)
C(6)	-0.0195 (15)	0.3690 (11)	0.5131 (11)	4.8 (10)	C(66)	0.2343 (18)	0.4383 (12)	0.3629 (12)	5.4 (11)
C(11)	-0.0968 (16)	0.2149 (13)	0.5344 (10)	4.7 (10)	B(1)	0.3675 (19)	0.3327 (15)	0.8701 (12)	4.6 (11)
C(12)	-0.0754 (20)	0.1237 (14)	0.5429 (14)	7.5 (13)	CA(1)	0.2847 (16)	0.2656 (12)	0.9103 (11)	4.2 (10)
C(13)	-0.1778 (25)	0.0938 (18)	0.5640 (17)	10.2 (18)	CB(1)	0.3239 (17)	0.1832 (12)	0.9645 (12)	5.0 (10)
C(14)	-0.2943 (25)	0.1560 (26)	0.5780 (17)	9.9 (19)	CC(1)	0.2507 (25)	0.1262 (14)	0.9977 (12)	6.4 (13)
C(15)	-0.3116 (22)	0.2430 (18)	0.5699 (17)	7.8 (16)	CD(1)	0.1418 (23)	0.1505 (17)	0.9711 (16)	6.9 (14)
C(16)	-0.2141 (19)	0.2759 (15)	0.5484 (12)	6.5 (12)	CE(1)	0.0960 (18)	0.2327 (15)	0.9209 (17)	7.9 (14)
C(21)	0.1283 (17)	0.1899 (11)	0.5785 (12)	6.5 (5)	CF(1)	0.1702 (15)	0.2925 (13)	0.8853 (12)	5.3 (10)
C(22)	0.0813 (17)	0.1962 (11)	0.6640 (12)	10.3 (7)	CA(2)	0.3642 (13)	0.3716 (13)	0.7665 (12)	4.5 (10)
C(23)	0.1568 (17)	0.1557 (11)	0.7265 (12)	16.6 (12)	CB(2)	0.3460 (18)	0.3231 (15)	0.7152 (14)	6.7 (13)
C(24)	0.2793 (17)	0.1089 (11)	0.7035 (12)	15.8 (11)	CC(2)	0.3549 (20)	0.3521 (18)	0.6277 (16)	7.0 (15)
C(25)	0.3263 (17)	0.1026 (11)	0.6180 (12)	22.4 (17)	CD(2)	0.3745 (19)	0.4305 (20)	0.5869 (15)	7.0 (15)
C(26)	0.2508 (17)	0.1431 (11)	0.5555 (12)	13.5 (10)	CE(2)	0.3917 (15)	0.4822 (15)	0.6374 (16)	6.2 (13)
C(31)	0.4109 (15)	0.2658 (12)	0.2681 (14)	4.8 (10)	CF(2)	0.3849 (13)	0.4531 (12)	0.7270 (12)	4.3 (10)
C(32)	0.4602 (18)	0.3215 (14)	0.2098 (15)	7.2 (13)	CA(3)	0.5109 (16)	0.2738 (11)	0.8800 (13)	4.7 (10)
C(33)	0.5614 (24)	0.3373 (20)	0.2257 (19)	9.0 (18)	CB(3)	0.5954 (16)	0.2451 (10)	0.8142 (11)	4.1 (9)
C(34)	0.6045 (27)	0.2996 (24)	0.3007 (28)	12.3 (26)	CC(3)	0.7178 (21)	0.1939 (15)	0.8237 (19)	7.9 (16)
C(35)	0.5567 (26)	0.2394 (22)	0.3576 (21)	12.1 (23)	CD(3)	0.7548 (24)	0.1732 (18)	0.9047 (24)	10.0 (19)
C(36)	0.4574 (19)	0.2219 (15)	0.3461 (17)	7.8 (15)	CE(3)	0.6689 (28)	0.1976 (19)	0.9760 (19)	10.2 (8)
C(41)	0.3619 (15)	0.1232 (11)	0.2271 (11)	4.0 (9)	CF(3)	0.5427 (20)	0.2552 (18)	0.9615 (16)	8.6 (16)
C(42)	0.4771 (16)	0.1077 (13)	0.1729 (11)	5.1 (10)	CA(4)	0.3181 (16)	0.4131 (12)	0.9230 (11)	4.6 (10)
C(43)	0.5295 (17)	0.0235 (13)	0.1406 (13)	5.4 (11)	CB(4)	0.3887 (19)	0.4616 (14)	0.9335 (15)	7.7 (13)
C(44)	0.4749 (21)	-0.0368 (13)	0.1659 (14)	5.8 (12)	CC(4)	0.3480 (23)	0.5299 (18)	0.9776 (17)	9.3 (17)
C(45)	0.3633 (20)	-0.0202 (12)	0.2215 (14)	6.8 (12)	CD(4)	0.2259 (25)	0.5606 (15)	1.0120 (15)	7.5 (15)
C(46)	0.3084 (18)	0.0586 (13)	0.2538 (13)	6.4 (12)	CE(4)	0.1530 (18)	0.5203 (15)	1.0019 (12)	5.2 (11)
C(51)	-0.0525 (16)	0.2009 (12)	0.2314 (13)	5.2 (10)	CF(4)	0.1974 (18)	0.4464 (12)	0.9596 (11)	5.0 (10)

^a Equivalent isotropic thermal parameters result from one-third of the trace of the anisotropic *B*_{ij} tensor. The esd's in the least significant figures are given in parentheses.

Table IV. Crystallographic Data for **3** (TB-5-23)

chiral [PtH(P ₄)](BPh ₄) (3)	<i>f</i> w 1186.06
<i>a</i> = 12.126 (3) Å	space group <i>P</i> $\bar{1}$ (No. 2)
<i>b</i> = 16.343 (4) Å	<i>T</i> = 21 °C
<i>c</i> = 16.390 (6) Å	λ = 0.71069 Å
α = 74.31 (3)°	ρ_{obsd} = 1.40 g cm ⁻³
β = 76.02 (2)°	ρ_{calcd} = 1.381 g cm ⁻³
γ = 67.38 (2)°	μ = 24.85 cm ⁻¹
<i>V</i> = 2851.72 Å ³	transm coeff = 0.81–0.99
<i>Z</i> = 2	<i>R</i> = 0.066, <i>R</i> _w = 0.061

4). This is a consequence of the steric requirements of nonplanar tetracoordinate forms of chiral P₄^{6c} and mainly due to the fact that the PhP–Pt–PPh₂ angles are forced to be smaller than 90°.²⁸

Discussion

Examination of molecular models of nonplanar tetracoordinate forms of chiral and *meso*-P₄ indicates that in contrast to chiral P₄, *meso*-P₄ comfortably adopts a nonplanar configuration.^{6c} As a consequence, a smooth movement along the square-planar to tetrahedral reaction coordinate is only possible in the case of tetracoordinate *meso*-P₄. Thus, no direct evidence for an intermediate between structural types **1** and **3** was obtained, which was the case for types **2** and **4** in solutions of **5**. However, the presence of a Berry-type rearrangement in a small amount in solutions of **3** is confirmed by its solid-state structure. Since the X-ray molecular structure of **3** is a strongly distorted trigonal bipyramid, an intermediate in the Berry mechanism different from a square pyramid and corresponding to the solution structure of **3** is possible.²¹ Though in [FeBr(P₄)](BPh₄), P₄ occupies both axial positions of a trigonal bipyramid,^{6f,j} the solid-state structure of **3** shows the energetically favored configuration with the hydride

ligand in an axial position. The same configuration is observed for the case of *meso*-P₄ in solutions of **5**. The intermediate in the Berry mechanism present in small amount in CD₃NO₂ solutions of **5** corresponds to structural type **4** with the solution structure of **3** being the other diastereomer. Both intermediate structures deviate from idealized Berry intermediates presumably causing the low amount of Berry rearrangement present. This is confirmed by the strongly increasing participation of the Berry mechanism occurring in acetone-*d*₆ solutions of **5**, which contain a flattened version of structural type **4** in better agreement with the square pyramid required for an idealized Berry rearrangement. The hydride ligand shows tetrahedral jumping in **1**, **2**, and **5**. The linking ethylene chains of P₄ lie closely along three of the six tetrahedral edges in a manner that all four tetrahedral faces are reachable for the hydride ligand by tetrahedral jumping, a mechanism with low rearrangement barriers.²¹

The steric requirements of P₄ destabilize its square-planar arrangement around a platinum(II) center.⁷ A complete destabilization of square-planar structures has been found for [PtClMe(*t*-Bu–N=CHCH=N–*t*-Bu)].^{8a} In the case of [PtClMe(6-Mepy–2-CH=N–(S)–CH(Me)Ph)] both a square-planar and a trigonal-bipyramidal species can be observed.²⁹ Several different nonplanar structures occur in platinum(II) complexes of P₄, as described above and reported previously.^{6a}

However, none of the above five-coordinate platinum(II) hydrides contains a planar tetradentate P₄ arrangement resulting in a square-pyramidal coordination geometry. Thus, an additional electronic effect, the high electron-releasing ability of the hydride ligand, completely destabilizes a planar P₄ coordination around a platinum(II) center leading to the different nonplanar P₄ ar-

(28) Brüggeller, P. Unpublished results.

(29) Albano, V. G.; Braga, D.; De Felice, V.; Panunzi, A.; Vitagliano, A. *Organometallics* 1987, 6, 517.

(30) Brüggeller, P. Unpublished results.

rangements in the five-coordinate platinum(II) hydrides reported in this paper.

Acknowledgment. I thank the MPI Martinsried, Munich, FRG, for making the use of a CAD4 diffractometer possible.

Supplementary Material Available: Listings of positional and thermal parameters, selected bond distances, bond angles, and torsion angles and a figure showing an ORTEP diagram (10 pages); a table of calculated and observed structure factors (28 pages). Ordering information is given on any current masthead page.

Contribution from the Department of Chemistry,
University of Florence, 50144 Florence, Italy

Synthesis, Crystal Structure, and Magnetic Properties of Tetranuclear Complexes Containing Exchange-Coupled Ln_2Cu_2 ($\text{Ln} = \text{Gd}, \text{Dy}$) Species

Cristiano Benelli, Andrea Caneschi, Dante Gatteschi,* Olivier Guillou, and Luca Pardi

Received May 31, 1989

By reacting CuSatnOH ($\text{CuSatnOH} = [N-(3\text{-aminopropyl})\text{salicylaldiminato}]\text{hydroxocopper(II)}$) with rare-earth hexafluoroacetylacetonates (hfac), complexes of general formula $\text{Ln}(\text{hfac})_3\text{CuSatnOH}$ ($\text{Ln} = \text{Gd}, \text{Dy}$) were obtained. The crystal structure of the dysprosium derivative was determined through X-ray diffraction at room temperature: the complex crystallizes in the triclinic system, space group $P\bar{1}$, with $a = 12.386$ (5) Å, $b = 13.574$ (3) Å, $c = 13.918$ (4) Å, $\alpha = 69.38$ (2)°, $\beta = 65.35$ (6)°, $\gamma = 69.93$ (5)°, and $Z = 2$. The gadolinium derivative was found to be isomorphous. The magnetic properties of both compounds and their EPR spectra are reported. The magnetic properties of the gadolinium derivative are discussed together with previous data reported in the literature, and a spin-polarization model is suggested to justify the observed ferromagnetic coupling between gadolinium and copper. The relevance of these data to the magnetic properties of high- T_c superconductors is also discussed.

Introduction

Exchange interactions involving transition-metal ions and rare-earth ions are relevant to many different scientific areas. In solid-state physics rare-earth ions have long been used to modulate the magnetic properties of spinels, orthoferrites, and garnets, taking advantage of their anisotropic properties.¹⁻¹³ In some cases new materials have also been developed for magnetic bubble memories^{14,15} and for magneto-optical devices.^{16,17} Somewhat related to this problem are also the novel high-technology magnets such as Sm_5Co and $\text{Nd}_2\text{Fe}_{14}\text{B}$.^{18,19}

Table I. Crystallographic Data and Experimental Parameters for $\text{Dy}(\text{hfac})_3\text{CuSatnOH}$

formula $\text{C}_{25}\text{H}_{17}\text{F}_{18}\text{N}_2\text{O}_8\text{DyCu}$	$Z = 2$
fw 1041.39	$\rho_{\text{calcd}} = 1.792 \text{ g cm}^{-3}$
cell params: $a = 12.386$ (5) Å, $b = 13.574$	$T = 18 \text{ }^\circ\text{C}$
(3) Å, $c = 13.971$ (4) Å, $\alpha = 69.38$ (2)°, β	$\lambda = 0.71069 \text{ Å}$
$= 65.35$ (6)°, $\gamma = 69.93$ (5)°, $V = 1936.66$	$R(F_o) = 0.0590$
(2) Å ³	$R_w(F_o) = 0.0590$

Another field of large interest is that of the new high- T_c superconductors of the $\text{YBa}_2\text{Cu}_3\text{O}_{7-x}$ type, where the substitution of Y with magnetic lanthanides does not vary the superconductive properties of the materials²⁰⁻²² while developing new interesting magnetic properties.²³⁻²⁵

Finally, fast relaxing lanthanide ions, such as dysprosium(III), have been used as relaxing agents for transition-metal complexes and also for metalloproteins in order to obtain structural information in solution.²⁶

All these studies demand that the basics of the interaction of the lanthanide ions with transition-metal ions be better understood, especially in order to establish useful structural-magnetic correlations of the types now rather well-known in the case of transition-metal ions.²⁷

- (1) Moskvina, A. S.; Bostrem, I. G. *Sov. Phys.—Solid State (Engl. Transl.)* **1977**, *19*, 1532.
- (2) Cooke, A. H.; Martin, D. M.; Wells, M. R. *J. Phys. C* **1974**, *7*, 3133.
- (3) Veltrusky, I.; Nekversie, V. *J. Phys. C* **1980**, *13*, 1685.
- (4) Cashion, J. D.; Cooke, A. H.; Martin, D. M.; Wells, M. R. *J. Phys. C* **1970**, *3*, 1612.
- (5) Foglio, M. E.; Van Vleck, J. H. *Proc. R. Soc. London, A* **1974**, *A336*, 115.
- (6) Wickersheim, K. *Phys. Rev.* **1962**, *122*, 1376.
- (7) Levy, P. M. *Phys. Rev. A* **1964**, *135*, 155.
- (8) Kadomtseva, A. M.; Bostrem, I. G.; Vasilieva, L. M.; Krynetskii, I. B.; Lukina, M. M.; Moskvina, A. S. *Sov. Phys.—Solid State (Engl. Transl.)* **1980**, *22*, 1146.
- (9) Goloventchis, E. I.; Sanina, V. A. *Sov. Phys.—Solid State (Engl. Transl.)* **1981**, *23*, 977.
- (10) Yamaguchi, T.; Tsushima, K. *Phys. Rev. B: Solid State* **1973**, *B8*, 5187.
- (11) Yamaguchi, T. *J. Phys. Chem. Solids* **1974**, *55*, 479.
- (12) Kadomtseva, A. M.; Lukina, M. M.; Moskvina, A. S.; Khafizova, N. A. *Sov. Phys.—Solid State (Engl. Transl.)* **1978**, *20*, 1235.
- (13) Washimiya, S.; Satoko, C. *J. Phys. Soc. Jpn.* **1978**, *20*, 1235.
- (14) Blunt, R. *Chem. Br.* **1983**, *19*, 740.
- (15) Nielsen, J. W. *IEEE Trans. Magn.* **1976**, *12*, 327.
- (16) Tsushima, T. In *Physics of Magnetic Materials*; Rauluszkiwicz, J., Szymczak, H., Lachowicz, H. K., Eds.; World Scientific: Singapore, 1985; p 479.
- (17) Hansen, P.; Hartmann, M. In ref 16, p 158.
- (18) Allibert, C.; Ballon, R.; Bley, F.; Deporter, J.; Gignox, D.; Givord, D.; Laforest, J.; Lemarie, R. In ref 16, p 283.
- (19) Sagawa, M.; Fujimura, S.; Togawa, M.; Yamamoto, H.; Matsura, Y. *J. Appl. Phys.* **1984**, *55*, 2083.
- (20) Hor, P. H.; Meng, R. L.; Wang, Y. Q.; Gao, L.; Huang, Z. J.; Bechtold, J.; Forster, K.; Chu, C. W. *Phys. Rev. Lett.* **1987**, *35*, 7238.
- (21) Murphy, D. W.; Sunshine, S.; Van Dover, R. B.; Cava, R. J.; Batlogg, B.; Zahnrak, S. M.; Schneemeyer, L. F. *Phys. Rev. Lett.* **1987**, *58*, 1888.
- (22) Tarascon, J. M.; McKinnon, W. R.; Greene, L. H.; Hull, G. W.; Vogel, E. M. *Phys. Rev.* **1987**, *B36*, 226.
- (23) Poddar, A.; Mandal, P.; Choudhury, P.; Das, A. N.; Ghosh, B. *J. Phys. C* **1988**, *21*, 3323.
- (24) Hodges, J. A.; Imbert, P.; Marinon da Cunha, J. B.; Hammann, J.; Vincent, E. *Physica B+C: (Amsterdam)* **1988**, *156*, 143.
- (25) Lynn, J. W.; Li, W. H.; Mook, H. A.; Sales, B. C.; Fisk, Z. *Phys. Rev. Lett.* **1988**, *60*, 2781.
- (26) Bertini, I.; Luchinat, C.; Messori, L. In *NMR of Paramagnetic Systems*; Sigel, H., Ed.; Marcel Dekker: Basel, Switzerland, 1987; p 21.
- (27) Willett, R. D.; Gatteschi, D.; Kahn, O., Eds. *Magneto-Structural Correlations in Exchange Coupled Systems*; Reidel: Dordrecht, The Netherlands, 1985.